

P7R.16 THE FREQUENCY OF OCCURRENCE OF QUASI-MONOCHROMATIC INERTIA-GRAVITY WAVES IN THE LOWER STRATOSPHERE FROM MST RADAR OBSERVATIONS

G.D. Nastrom^{*+} and F.D. Eaton[@]

⁺St. Cloud State University, St. Cloud, Minnesota

[@]Air Force Research Laboratory, Albuquerque, New Mexico

1. INTRODUCTION

Quasi-monochromatic oscillations with periods near the inertial period have been found in a wide variety of measurements in the lower stratosphere. Vertical profiles of wind and/or temperature from radiosondes have a long history of use for such studies (e.g., Madden and Zipser, 1970; Thompson, 1978; Vincent and Alexander, 2000; Sato, et al., 2003; Tsuda, et al., 2004; Zhang and Yi, 2005, among many others) and are sometimes used over broad areas (e.g., Wang, et al., 2005). Constant density balloon trajectories in the lower stratosphere also have shown persistent near-inertial wave patterns (Hertzog, et al., 2002). The advent of wind profiler radars has made it possible to examine both the vertical and temporal structure of such oscillations with high resolution (e.g., Sato and Woodman, 1982; Cornish and Larsen, 1989; Sato, 1989, 1994; Riggins, et al., 1995; Sato, et al., 1999; Serfinovich, et al., 2005). However, as noted by Fritts and Alexander (2003), radar studies except at the MU radar in Japan have been limited to short-term campaigns. For example, Nastrom and Eaton (2003) recently noted the presence of a strong oscillation in a week of wind observations from Vandenberg Air Force Base, California (VBG). The purpose of this study is to use the entire set of observations available from the 50 MHz wind profiler (MST) radars at VBG and at White Sands Missile Range, New Mexico (WSMR), to examine the frequency of occurrence of near-inertial period quasi-monochromatic wind oscillations.

2. RESULTS

Wind observations from WSMR are available from 1991-1996 (Hansen, et al., 2001). The radar was relocated to VBG where observations are available for 2001-April 2004.

*Corresponding author: Dr. Gregory D. Nastrom, Dept. of Earth and Atmospheric Sciences, St. Cloud State Univ., St. Cloud, MN 56301-4498. e-mail: gdnastrom@stcloudstate.edu

In the example shown by Nastrom and Eaton (2003), the oscillation has a vertical wavelength of a few km, a period near the inertial period (the inertial period is 21.04 hours at VBG and 22.40 at WSMR), amplitude of several m/s, and appears to be unrelated to the flow in the troposphere. These features are consistent with those noted by Cornish and Larsen (1989). Similar features are apparent during many days in the time-height series of wind observations from WSMR during June-August, 1994, shown in Figure 1. The corresponding plots for other summers (not shown) are similar. However, examination of such plots for mid-winter months rarely show clear examples of quasi-monochromatic near-inertial oscillations, implying the fraction of the total wind variance contained in near-inertial frequencies is significantly reduced during winter.

Power spectral analyses were used to explore the cause of this relative reduction in variance. The entire data series of hourly mean zonal and meridional winds at each altitude was divided into 128-hour segments. Hours with fewer than five observations that passed quality control checks were set to missing, except linear interpolation was used to fill gaps up to two hours. Segments with data gaps more than two hours wide were not retained for spectral analysis. A fast Fourier transform (FFT) algorithm was used to estimate spectral powers of the residuals from a linear trend line fit to each 128-hour data segment. The spectra were smoothed with a Hanning filter. Average spectra for all segments at WSMR during June through September (JJAS) and December through March (DJFM) are given in Figure 2. A reference line with slope $-5/3$ is placed at the same coordinates in each panel to aid comparisons. The spectra for zonal and meridional winds are very similar. The high frequency portions of these spectra (above about 2×10^{-5} Hz) closely follow a $-5/3$ slope, especially in the stratosphere. Near the inertial frequency (1.24×10^{-5} Hz) there is enhanced energy relative to an extrapolation of a $-5/3$ line from the higher frequencies, especially in the stratosphere during JJAS. Nastrom, et al.

(1997) hypothesized an enhancement of wave activity at near-inertial frequencies.

The total wind variance (zonal plus meridional) spectra are given in Figure 3. The area-preserving coordinates used in Figure 3 emphasize the relative enhancement of energy near the inertial frequency in the stratosphere during summer. Note that the relative enhancement is smaller during winter than during summer; as a result the probability of seeing a quasi-monochromatic oscillation is largest in the stratosphere during summer.

The following procedure was used to quantify the probability of seeing a quasi-monochromatic oscillation. Blocks of hourly-mean zonal and meridional winds 72 hours long by 13 levels (i.e., 1.95 km) in the vertical were fit with waves as $\exp[i(mz-\omega t)]$, where the vertical wavenumber $m=2\pi/\lambda_z$, the vertical wavelength, and $\omega=2\pi/P$, the period. The combination of λ_z (1 to 6 km), P (16 to 24 hours), and lag between zonal and meridional winds (0 to P hours) that maximized the percent of explained variance (PEV) was found for each data block. PEV is defined as $100(r_u^2\sigma_u^2+r_v^2\sigma_v^2)/(\sigma_u^2+\sigma_v^2)$. As this analysis was made using 72-hour data blocks at 24-hour intervals, the results are not all independent. A data block was retained for analysis only if 60 or more hours had observations at 8 or more levels. The entire time series at each level for each wind component was first low-pass filtered with a 5-point binomial filter. The residuals from a linear trend fit to each 72-hour data segment at each level were used for the wave-fitting analysis. The analyses were made for six altitude blocks, centered at 13.5, 14.5, ..., 18.5 km. The number of data blocks retained for analysis at each altitude was 654, 699, 715, 722, 727, and 724 at WSMR, and 338, 343, 330, 292, 249, and 142 at VBG. An example of the fitting is given in Figure 4; note there are a few missing data points so the number used for fitting (# obs=897) is less than the total possible (936). The best-fit values for the case in Figure 4 are $P=21$ hr and $\lambda_z=4.75$ km; with $PEV=0.58$. The equivalent wave amplitude, $A=2^{1/2}\sigma$, is 5.1 (4.7) m/s for u (v).

The annual distribution of PEV at WSMR (VBG) is given in the upper left panel of Figure 5 (Figure 6). PEVs are generally enhanced during the summer, relative to winter. A quasi-monochromatic oscillation seems to be present when the PEV is above about 0.25. For example, the lower left panels of Figures 5 and 6 show the distributions of σ_u^2/σ_v^2 as functions of PEV; this ratio settles down to values near one

for $PEV>0.25$. Other variables (not shown) also suggest $PEV>0.25$ as a threshold for quasi-monochromatic oscillations. Figure 7 shows the percent of cases with $PEV>0.25$ as a function of month and height at WSMR; the summer stratospheric maximum is striking.

Most cases of $PEV>0.25$ are associated with wind speeds less than about 10 m/s (upper right panels of Figures 5 and 6). However, it is possible that this relationship is coincidence, and not causative; i.e., light winds and large PEV both just happen to occur in summer. No apparent relationship of PEV with vertical shear of the horizontal wind was found.

A large number of gravity wave variables can be derived from the fitted values of λ_z , P , and lag between u and v (following, e.g., Sato, et al., 1997). For example, the lower right panels of Figures 5 and 6 show the ratios of the intrinsic frequencies, ω_i , to the Coriolis parameter, f , as functions of PEV. The values range between about 2 and 3, consistent with the values reported by Wang, et al. (2005) from their analyses of high-resolution radiosondes. Further analyses of the radar data will be reported elsewhere.

3. SUMMARY

Hourly mean winds from the 50 MHz MST radars at WSMR and VBG have been used to study the occurrence of quasi-monochromatic oscillations. Spectral analysis shows there is a strong enhancement of wave energy near the inertial frequency, especially in summer in the stratosphere. This enhancement explains why many case studies and brief campaigns have been more likely to note apparent low frequency waves in summer than in winter.

A climatology of the occurrence of quasi-monochromatic oscillations has been developed by fitting blocks of data over 72 hours and 1.95 km with sinusoids. It is found that a single sinusoid explains over 25 percent of the total wind variance in more than 50 percent of the cases at WSMR during summer in the stratosphere. The probability of finding a case of $PEV>0.25$ is small at all heights in winter.

4. REFERENCES

Cornish, C.R., and M.F. Larsen, 1989: Observations of low-frequency inertia-gravity waves in the lower stratosphere over Arecibo, J. Atmos. Sci., 46, 2428-2439.

Fritts, D.C. and Alexander, M. J., 2003: Gravity wave dynamics and effects in the middle atmosphere, Rev. Geophys., vol.41, No.1, doi:10.1029/2001RG000106.

Hansen, A. R., G.D. Nastrom, Eaton, F.D., 2001: Seasonal variation of gravity wave activity at 5 – 20 km observed with the VHF radar at White Sands Missile Range, New Mexico, J. Geophys. Res., 106, 17171-17183.

Hertzog, A., F. Vial, C.R. Mechoso, C. Basdevant, and P. Cocquerez, 2002: Quasi-Lagrangian measurements in the lower stratosphere reveal an energy peak associated with near-inertial waves. Geophys. Res. Lettr., 29, No. 8, doi: 10.1029/2001GL014083.

Madden, R.A., and E. J. Zipser, 1970: Multi-layered structure of the wind over the equatorial Pacific during the Line Islands experiments. J. Atmos. Sci., 27, 336-343.

Nastrom, G.D., T.E. VanZandt, and J.M. Warnock, 1997: Vertical wavenumber spectra of wind and temperature from high-resolution balloon soundings over Illinois. J. Geophys. Res., 102, 6685-6701.

Nastrom, G.D., and F. D. Eaton, 2003: A case study of atmospheric conditions at 4-19 km over Vandenberg AFB during passage of a cyclone. J. Appl. Meteor., 42, 467-475.

Riggin, D. D.C. Fritts, C.D. Fawcett, and E. Kudeki, 1995: Observations of inertia-gravity wave motions in the stratosphere over Jicamarca, Peru. Geophys. Res. Lettr., 22, 3239-3242.

Sato, K., 1989: An inertial gravity wave associated with a synoptic-scale pressure trough observed by the MU radar. J. Met. Soc. Japan, 67, 325-333.

Sato, K., 1994: A statistical study of the structure, saturation and sources of inertia-gravity waves in the lower stratosphere observed with the MU radar. J. Atmos. Terr. Phys., 56, 755-774.

Sato, K., D. J. O'Sullivan, and T.J. Dunkerton, 1997: Low-frequency inertia-gravity waves in the stratosphere revealed by three-week continuous observation with the MU radar. Geophys. Res. Lettr., 24, 1739-1742.

Sato, K., T. Kumakura, and M. Takahashi, 1999: gravity waves appearing in a high-resolution GCM simulation. J. Atmos. Sci., 56, 1005-1018.

Sato, K. M. Ymamori, S.-Y. Ogino, N. Takahashi, Y. Tomidawa, and T. Yamanouchi, 2003: A meridional scan of the stratospheric gravity wave field over the ocean in 2001. J.

Geophys. Res., 108, No. D16, doi: 10.1029/2002JD003219.

Sato, T.S., and R.F. Woodman, 1982: Fine altitude resolution radar observations of upper-tropospheric and lower-stratospheric winds and waves. J. Atmos. Sci., 39, 2539-2545.

Serfinovich, A., P. Hoffmann, D. Peters, and V. Lehmann, 2005: Investigation of inertia-gravity waves in the upper troposphere/lower stratosphere over Northern Germany observed with collocated VHF/UHF radars. Atmos. Chem. Phys., 5, 295-310.

Thompson, R.O.R.Y., 1978: Observations of inertial waves in the stratosphere. Quart. J. R. Meteor. Soc., 104, 691-698.

Tsuda, T., M. V. Ratnam, P. T. May, M. J. Alexander, R. A. Vincent, and A. MacKinnon, 2004: Characteristics of gravity waves with short vertical wavelengths observed with radiosonde and GPS occultation during DAWEX (Darwin Area Wave Experiment), J. Geophys. Res., 109, D20S03, doi:10.1029/2004JD004946.

Vincent, R.A., and M.J. Alexander, 2000: Gravity waves in the tropical lower stratosphere: An observational study of seasonal and interannual variability. J. Geophys. Res., 105, 17,971-17,982.

Wang, L., M.A. Geller, and M.J. Alexander, 2005: Spatial and temporal variations of gravity wave parameters. Part I: Intrinsic frequency, wavelength, and vertical propagation direction, J. Atmos. Sci., 62 (1), 125-142.

Zhang, S.D., and F. Yi, 2005: A statistical study of gravity waves from radiosonde observations at Wuhan (30N, 114E) China. Ann. Geophys. 23, 665-673.

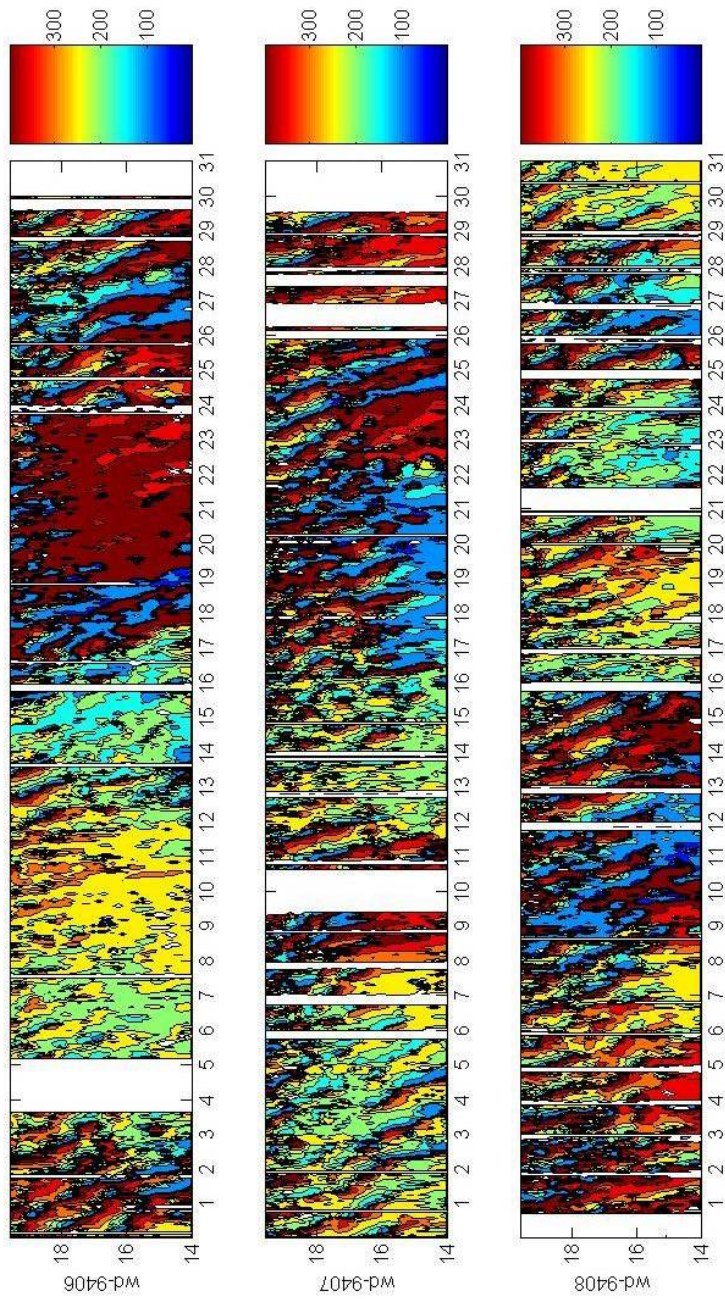


Figure 1. Time-height series of hourly mean wind directions at WSMR for June, July, and August, 1994. Missing data are blank. Note the apparent oscillations with periods slightly less than one day and which seem to propagate downward with time, especially clearest at the highest altitudes.

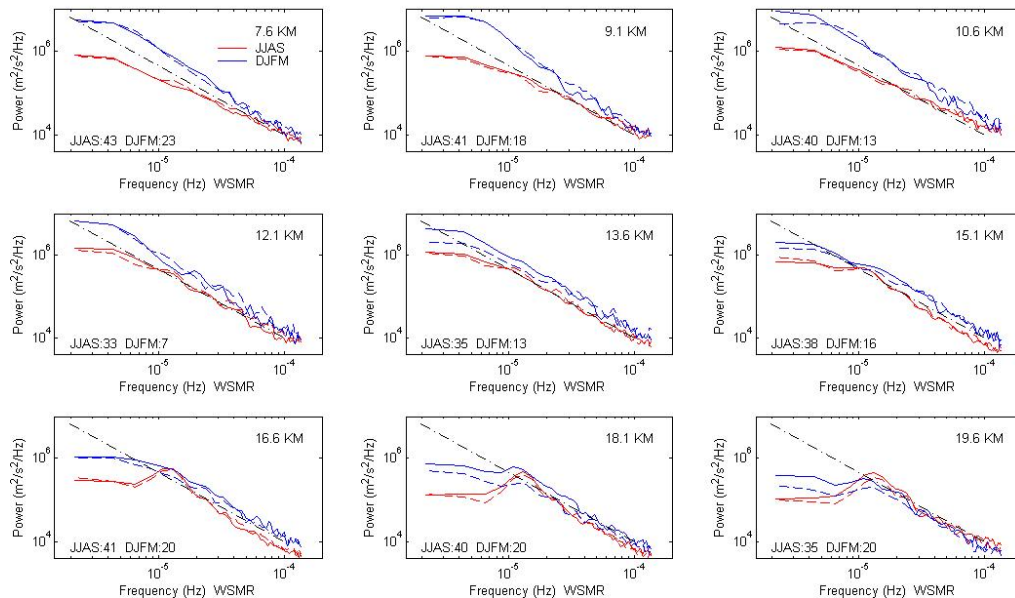
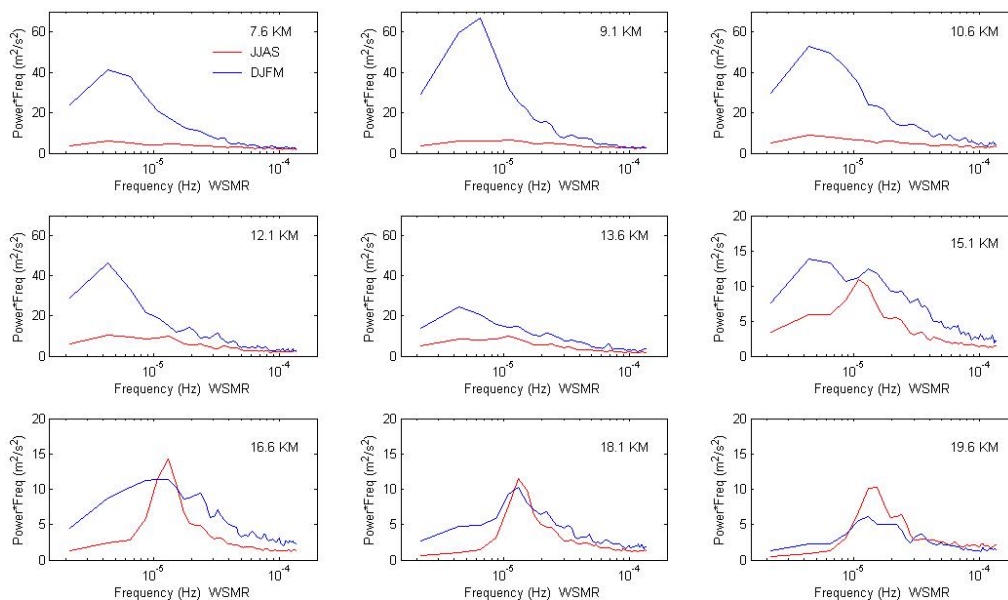


Figure 2. Frequency power spectra at WSMR for June-September (JJAS) and December-March (DJFM). A reference line with slope $-5/3$ is entered at the same coordinates in each panel. The number of individual spectra averaged for each curve is shown in the lower left corner of each panel. Solid: zonal winds; dashed: meridional winds.



c:\WSMR\inertial-05\spect128p.m 22-Aug-2005

Figure 3. As in Figure 2, except for total energy ($u+v$) in area preserving coordinates.

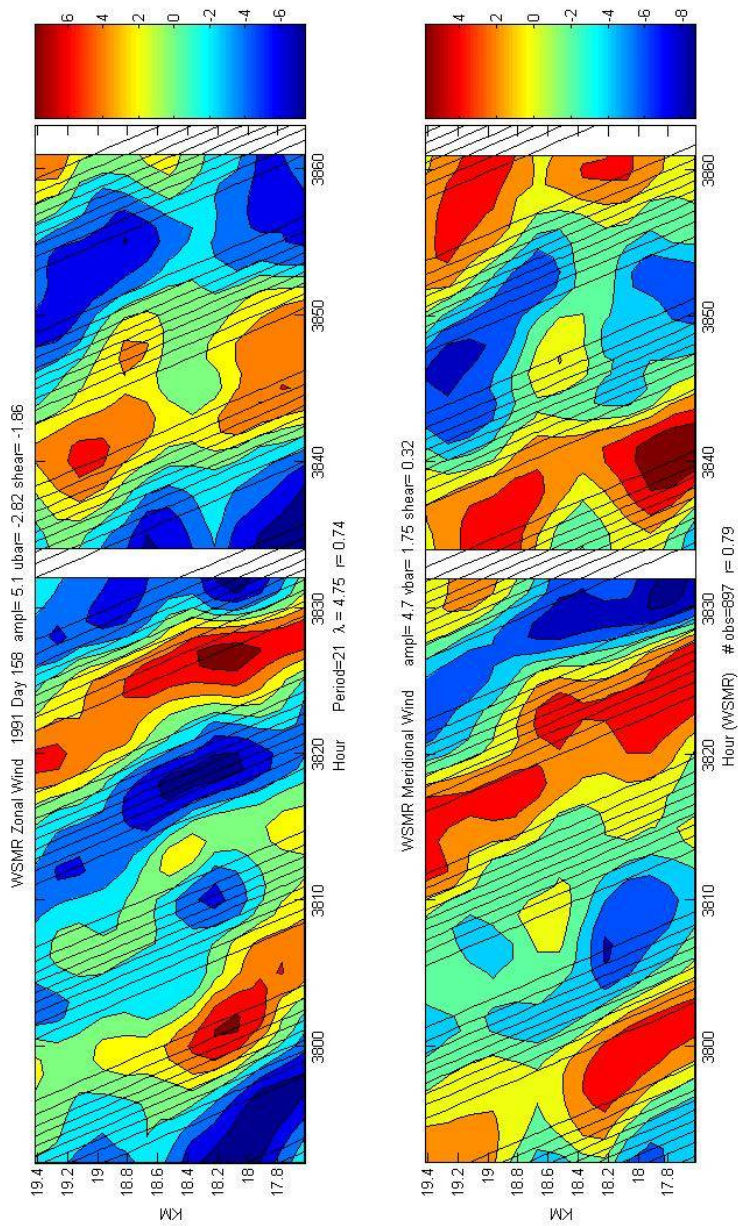


Figure 4. Example of winds for one 72-hour by 13-level data block at WSMR (upper: zonal, lower: meridional). This case begins on June 8, 1991. The best-fit function of the form $\exp[i((mz-\omega t))]$ is shown by the solid lines in arbitrary units. See text.

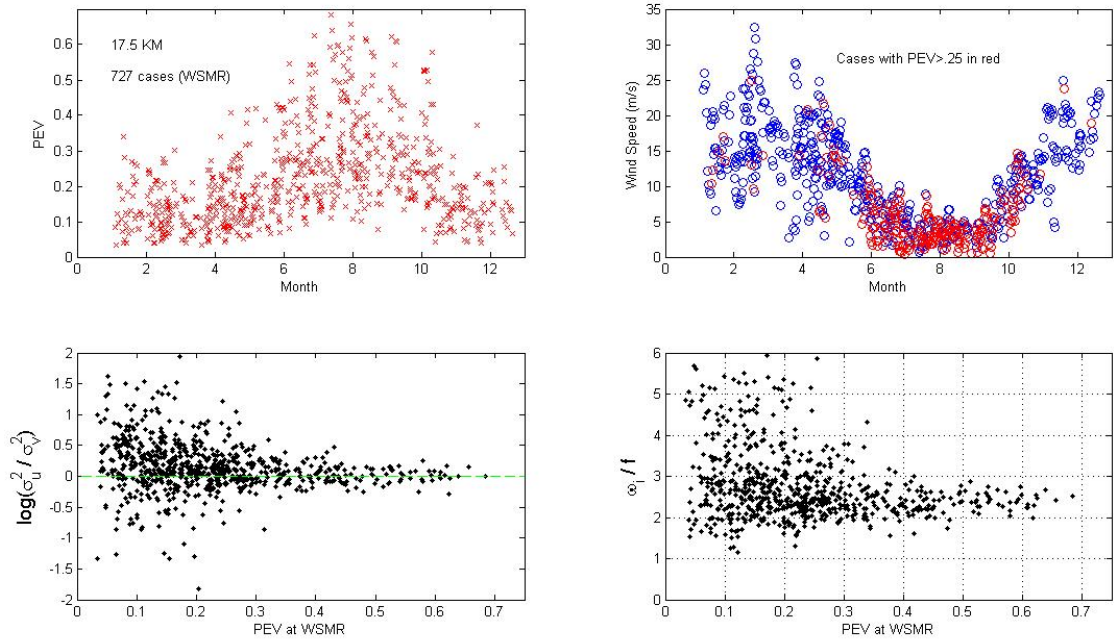


Figure 5. Results at 17.5 km at WSMR. (upper left) PEV as a function of time of year. (upper right) Wind speed as a function of time of year; data blocks with PEV>0.25 are shown in red. (lower left) Ratio of variance within individual data blocks of zonal wind to that of meridional wind as a function of PEV. (lower right) Ratio of intrinsic wave frequency to f as a function of PEV.

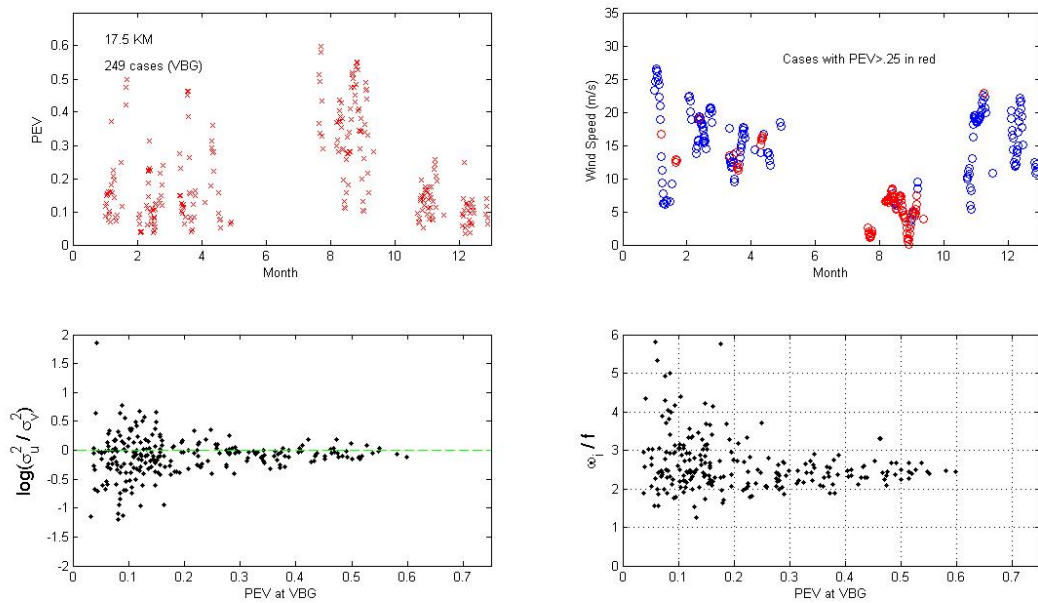


Figure 6. As in Figure 5, except at VBG.

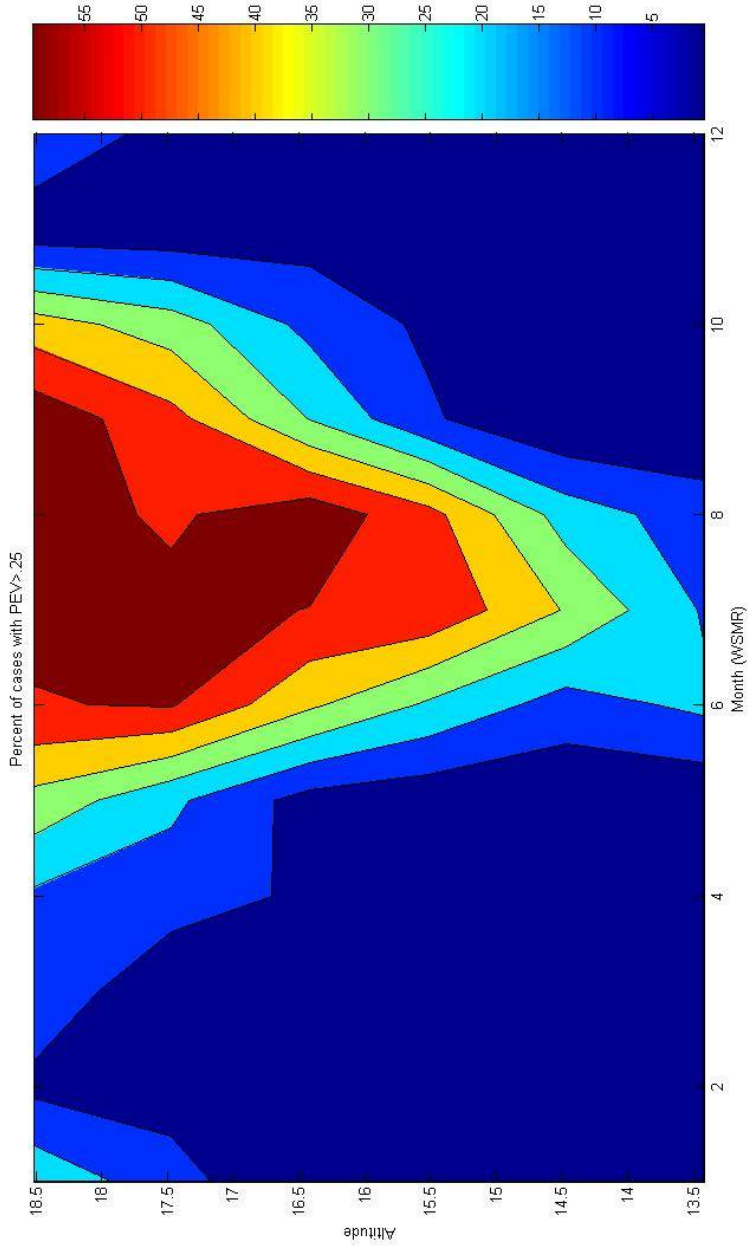


Figure 7. Month vs. height plot of the percent of cases with $PEV > 0.25$ at WSMR.